



Accurate low DOF modeling of a planar compliant mechanism with flexure hinges: the equivalent beam methodology

B. Zettl, W. Szyszkowski*, W.J. Zhang

Department of Mechanical Engineering, University of Saskatchewan, 57 Campus Drive, Saskatoon, SK, Canada S7N 5A9

Received 16 February 2004; received in revised form 28 June 2004; accepted 15 September 2004

Abstract

A methodology for accurate and efficient finite elements method (FEM) simulations of planar compliant mechanisms with flexure hinges is presented. First, using symmetry/antisymmetry boundary conditions and 3D elements, one-eighth of a single hinge is simulated to determine its true stress/stiffness characteristics. A set of fictitious beams is derived, which have the identical characteristics. This set is used in conjunction with other beams that model relatively stiff links to generate an equivalent model of an entire mechanism consisting of the beam elements only. The model has a low number of degrees-of-freedom (DOF) and appears to be more accurate than any 2D FEM models, even those with very large number of DOF. The methodology has been developed specifically for the right circular flexure hinge; however, it can be applied to all types of revolute flexure hinges.

© 2004 Elsevier Inc. All rights reserved.

Keywords: Compliant mechanisms; Flexure hinges; Finite element simulation

1. Introduction

The implementation of compliant mechanisms is common in modern micro-positioning systems and MEMS devices. Unlike conventional mechanisms, compliant mechanisms are monolithic structures that provide the required motion by way of flexure hinges inherent to the structure. The flexure hinges are placed between relatively rigid members, referred henceforth to as links, to provide the desired planar motion of the mechanism, typically driven by high accuracy actuators. This paper considers a mechanism with right circular hinges; however, the proposed methodology is applicable to planar mechanisms containing any of the revolute flexure hinge types.

An accurate FEM simulation of such mechanisms, despite the recent progress in computational techniques, still poses a challenge. Typical modern hinges should have relatively high depth-to-height ratios to maximize flexibility and secure

planar motion. The problem is that the stress and strain components in such hinges vary in the direction perpendicular to the plane of motion of the mechanism (across the hinge's thickness). This variation and its effect on the hinge's performance can only be analyzed with the use of 3D elements. However, the 3D FEM analysis (with a sufficient number of elements across the depth) even for one hinge requires thousands of elements. Such an analysis is reported in [1], despite a rather significant computational effort, the stress/strain variation across the hinge's thickness is not sufficiently depicted in the results.

There are numerous publications, inspired possibly by the planar mechanism's behavior, which use 2D plain stress elements [2–5] to model either a whole compliant mechanism or a flexure hinge thereof. Even the shell elements have been used in [6], which are difficult to justify for this particular application, since only their in-plane stiffness is utilized (which is identical to the stiffness of 2D plane stress elements). The shell element's out-of-plane bending capacity and the corresponding DOF (always zero) stay unused, which further invalidate the use of this element for modeling flexure hinges.

* Corresponding author. Tel.: +1 306 966 5440; fax: +1 306 966 5427.
E-mail address: szyszkow@engr.usask.ca (W. Szyszkowski).

As explained later in this paper any 2D model carries a systematic error, the magnitude of which depends mainly on the hinge's depth-to-height ratio.

On the other hand, the links between hinges of most of the compliant mechanisms are relatively stiff structural members. The strain/stress states in such members are very similar to that assumed in the standard beam elements, which can be referred to as 1D elements (as deformations due to only one stress component is considered). Therefore, the links require neither 3D nor 2D elements, since comparable modeling accuracy can be obtained from 1D beam elements with a significantly reduced numerical effort.

In the early works also circular hinges were approximated as beams in bending. In [7] the hinge's stiffness was determined analytically using the classical Euler–Bernoulli beam equation (the same equation is used in the above mentioned beam elements). In spite of a rather rudimentary character of such an approach the formulas derived in this work (known as the Paros–Weisbord stiffness formulas) are still used to provide a preliminary prediction of the hinge behavior [8,9].

This paper demonstrates the development and use of an accurate and numerically efficient model of a compliant mechanism, which combines the 3D characteristics of the hinges and the 1D characteristics of the links. The properties of the hinges are first determined from a separate 3D FEM model. These properties, via the use of some equivalent beams, are then incorporated into the model of the entire mechanism. The model consists of the beam elements only and is characterized by a small number of DOF, but is capable of simulating the mechanism's static and dynamic behaviors with accuracy that otherwise would require a large number of 3D elements and a significant computational effort. Clearly, such models should allow the use of the FEM simulation technique to its fullest capacity. The discussion of the methodology is focussed on a positioning device known as the 3RRR mechanism, which is presented in the next section.

2. The compliant mechanism

A circular end-effector of the 3RRR compliant mechanism is driven by three piezoelectric actuators attached to its base. As shown in Fig. 1, there are four flexure hinges and four links between each actuator the end-effector. The mechanism and the end-effector are capable of motion in the x – y plane. The nominal data for dimensions (which can be easily modified to include machining imperfections as discussed in [9], for example) and for material properties will be used in the computer simulations presented.

The thickness of the hinges and links is 10 mm (the whole mechanism has been fabricated out of a 10 mm thick plate). This dimension, in terms of the hinge geometry, is usually referred to as depth. Since its minimum height is 0.8 mm, the depth-to-height ratio for this particular hinge is 12.5. The height of the links is also 10 mm, while the radius of the

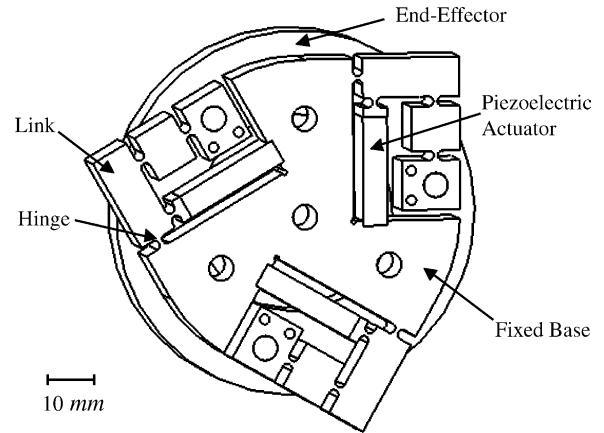


Fig. 1. Piezo-actuated compliant mechanism.

hinge is 1 mm. The material properties are given by Young's modulus $E = 105$ GPa, and Poisson's ratio $\mu = 0.33$.

As previously mentioned, despite the planar motion of the mechanism, the stress and strain components vary through the hinge's depth necessitating a 3D analysis. However, such an analysis of the whole mechanism would be numerically prohibitive. On the other hand, any analysis that applies 2D elements, though numerically feasible, ignores the above effects. Namely, either the stress or the strain in the depth directions is omitted in the 2D plane stress or plane strain elements, respectively. Nevertheless, such analyses are considered useful, since either the lower (plane stress) or the upper (plane strain) limits of the structure overall stiffness can be obtained. In this case they will be used to verify the equivalent beam model discussed in Section 4. The first step in building such a model is to determine the properties of the single hinge. Here this is done using 3D elements discussed next.

3. The hinge

Flexure hinges have been extensively studied using analytical and numerical methods. As already mentioned, the seminal analytical work [7] modeled the right circular flexure hinge as a beam in bending, which is essentially a 1D approximation. The bulk of FEM analyses have been done applying 2D plane stress elements [2–6]. A detailed 3D analysis of the hinge has been reported in [10]. Here only the model and the relevant results of this work are briefly outlined.

The hinge geometry (see Fig. 2a) is defined in terms of depth $b = 10$ mm, height $t = 0.8$ mm, and radius $r = 1$ mm. The link is defined by its height $h = 10$ mm and length $l = 9$ mm. The latter dimension was chosen such that the effects of hinge on the stress/strain distribution in the link disappear. The load is in the form of the bending moment of $M_z = 200$ N mm. Since the hinge has two planes of symmetry and one plane of antisymmetry, only one-eighth of it needs to be modeled. The 20-node brick elements, SOLID95 from the ANSYS pro-

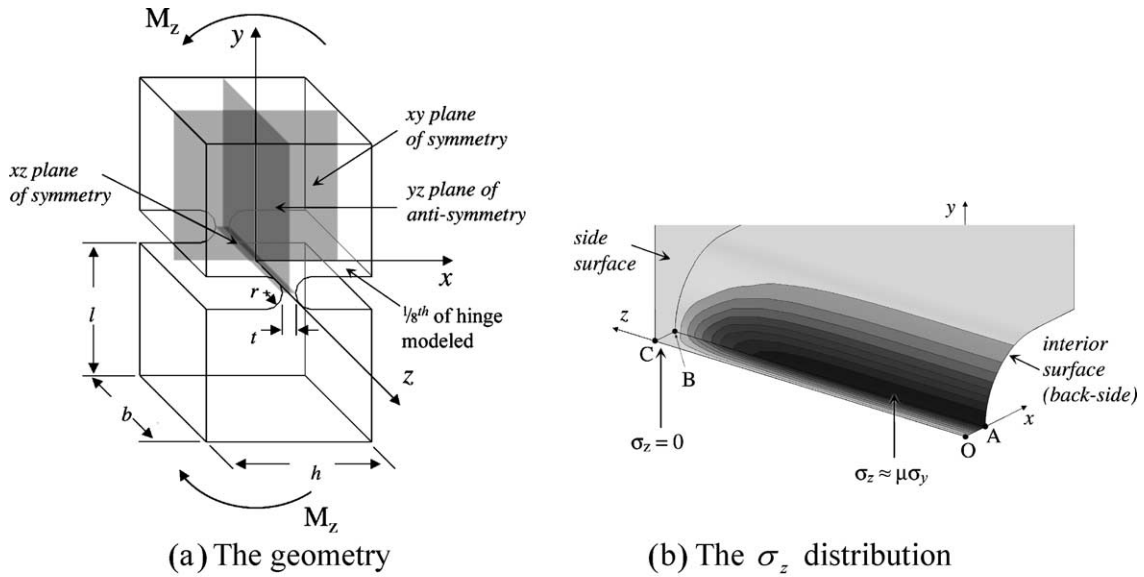


Fig. 2. (a) and (b) The Hinge modeled by 3D FEM elements; (c) deflection along hinge length.

gram, were used in the analysis. A satisfactory numerical accuracy was achieved with about 24 000 DOF.

The 3D nature of the stress/strain state is illustrated in Fig. 2b by the distribution of σ_z (the normal stress in the z -direction), where the dark shading indicates the area of high stress, and the light shading indicates the area of negligible stress. As seen, the plane stress condition ($\sigma_z = 0$) is met only at the free surface (for $z = 0.5b$), while the plane strain condition (represented by the relation $\sigma_z = \mu\sigma_y$) is satisfied for the prevailing part of the hinge. The maximum value of the stress σ_y was 219.3 MPa. This value will be used later in Section 4 to develop an equivalent beam model of the hinge.

The deformation pattern, represented by the lateral displacement v_x of the nodal points along the y -axis is shown

in Fig. 2c. A careful analysis of this plot reveals that for $y \geq r = 1$ mm the slope of the deflected model is the same (five significant digits of the results were compared). Therefore, the slope α and the deflection v_x (for convenience, positive as shown in the figure) calculated at $y = r$, are considered to be representative of the hinge flexibility.

Similar analyses have been performed for the hinges with different depths b .

The hinge's stiffness parameters are defined by:

$$k_\alpha^{3-d} = \frac{M_z}{b\alpha} \quad \text{and} \quad k_v^{3-d} = \frac{M_z}{bv_x} \quad (1)$$

The subscripts α and v indicate the rotational and lateral stiffness parameters, respectively, while the superscript 3-d

refers to the 3D model (for example, for $b = 10$ mm the numerical values of these parameters are $k_{\alpha}^{3-d} = 7823$ N and $k_v^{3-d} = 12010$ N/mm). This notation is used to distinguish between the results obtained from the 3D analysis and the corresponding 2D models. Such models were obtained by preserving the geometry of nodes on the 3D model in the x - y plane, and by using 8-nodes 2D elements (PLANE82). These elements can be applied with either the plane stress or the plane strain options. The 2D model had 1050 DOF (about 23 times less than the 3D model).

It is worthwhile to notice that for the 2D analyses the stiffness parameters (1) are independent of the hinge depth. However, for the 3D model their values vary with the depth-to-height ratio, as shown in Fig. 3 for the rotational stiffness (almost identical variation can be obtained for the lateral stiffness). The stiffnesses obtained from the 2D models are indicated by the superscripts ε for the plane strain and σ for the plane stress, respectively. The numerical values of these parameters are $k_{\alpha}^{\sigma} = 7100$ N, $k_{\alpha}^{\varepsilon} = 7968$ N, and $k_v^{\sigma} = 11052$ N/mm, $k_v^{\varepsilon} = 12223$ N/mm. For comparison, the corresponding values obtained from the 1D Poros–Weiborg formulas in [7] are $k_{\alpha} = 8503$ N and $k_v = 8503$ N/mm, which differ by about +8 and -29% respectively from the corresponding stiffnesses obtained from the 3D model. As can be seen, especially the lateral stiffness obtained from the 1D model is not particularly accurate. Note that the stiffnesses obtained from the plane stress analysis always underestimate, while stiffnesses from the plane strain analysis overestimate the stiffnesses obtained from the 3D model (i.e. $k^{\sigma} < k^{3d} < k^{\varepsilon}$). Moreover, since theoretically $k^{\sigma}/k^{\varepsilon} = 1 - \mu^2$ one can conclude that the potential systematic error of any 2D analysis may be up to about 12% (for $\mu = 0.33$) as indicated in Fig. 3.

On the other hand, the modeling error of the 2D analysis with the plane stress assumption should be less than 2% for

the hinges with the ratio $b/t < 2$ (domain I in the plot). Similarly, the error should not exceed 2% if the 2D plane strain elements are used for the hinges with the ratio $b/t > 12.5$ (domain III). Therefore flexure hinges that fall into domain I or III may be modeled by proper 2D elements. Such hinges can be considered ‘thin’ or ‘thick’, respectively. Also, it is interesting that for a given M_z the maximum stress, σ_y , obtained from both 2D models is always slightly lower (about 2%) than from the 3D model. This is due to the fact that, while producing the same resultant bending moment, this stress component is assumed constant across the hinge’s thickness in 2D models and varies in the 3D model.

4. The equivalent beam model for the hinge

For the purpose of modeling and simulation of its flexibility the hinge analyzed in the previous section is characterized by the ‘normalized’ rotational and lateral stiffnesses denoted as K_{α} and K_v respectively, where:

$$K_{\alpha} = \frac{k_{\alpha}^{3-d} b}{E} \quad \text{and} \quad K_v = \frac{k_v^{3-d} b}{E} \quad (2)$$

A third parameter can be added for the purpose of design to represent the maximum stress developed in the hinge due to moment M_z . Such a parameter, referred to as the hinge’s bending modulus, is defined as:

$$S = \frac{M_z}{\sigma_{\max}} \quad (3)$$

Here the three hinge parameters are assumed to be determined from the 3D FEM model. These parameters can also be obtained by other means, for example, from experiment. Also, the planar hinges of different shapes and types can be characterized by such parameters.

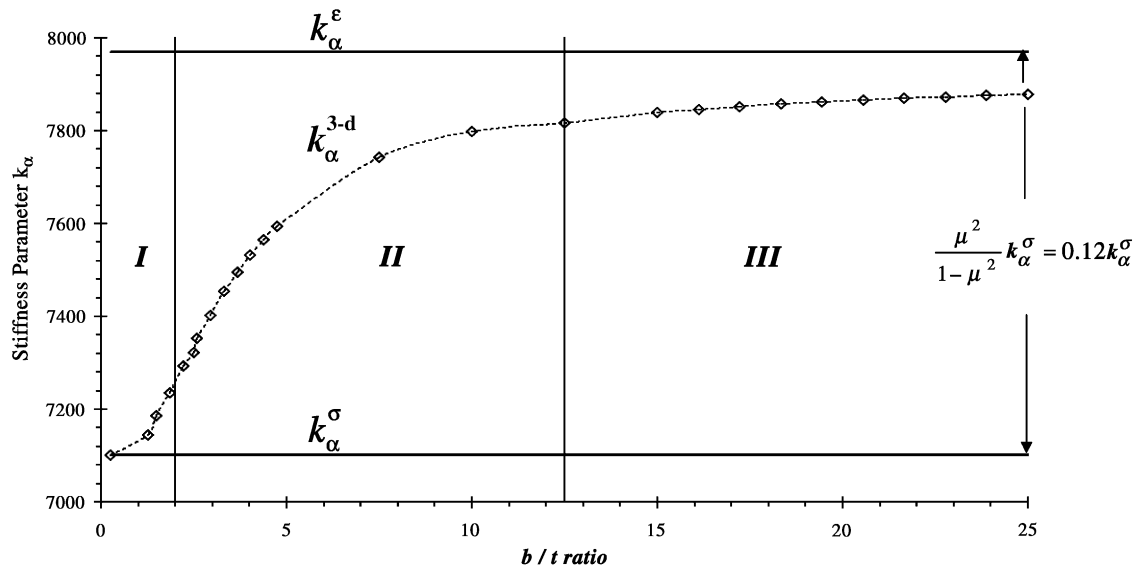


Fig. 3. Effect of the depth-to-height ratio on the rotational stiffness.

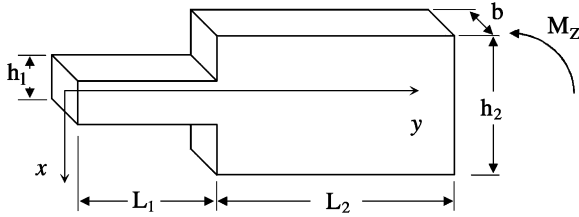


Fig. 4. Parameters defining the equivalent beam geometry.

Now, consider a beam of the shape shown in Fig. 4, made of the same material as the hinge. The beam is fixed at the end $y = 0$ and loaded by moment M_z . Assume that the beam's depth is b , and its total length is the same as the length of half of the hinge, i.e.:

$$L_1 + L_2 = r \tag{4}$$

The beam's behavior can be completely determined only if the values of the three parameters h_1 , h_2 and L_1 are known. These parameters can be defined in such a way that the beam response to the moment M_z is identical to the response of the hinge.

The beam's slope α at $y = r$ is found to be:

$$\alpha = \frac{M_z}{E} \left(\frac{L_1}{I_1} + \frac{L_2}{I_2} \right) = \frac{M_z}{K_\alpha E} \tag{5}$$

where $I_1 = bh_1^3/12$ and $I_2 = bh_2^3/12$.

The lateral deflection v_x at the same point is:

$$v_x = \frac{M_z}{2E} \left[\frac{L_1(2L_2 + L_1)}{I_1} + \frac{L_2^2}{I_2} \right] = \frac{M_z}{K_v E} \tag{6}$$

Assuming that the bending stress at the section $y = 0$ of the beam is to represent the hinge's maximum stress, i.e.: $\sigma_{y=0} = (M_z/I_1)(h_1/2) = \sigma_{\max}$, one obtains:

$$\frac{2I_1}{h_1} = S \tag{7}$$

It should be emphasized that stresses at other points of the beam (i.e.: for $y > 0$) are irrelevant.

The set of Eqs. (4)–(7) allow the parameters of the beam to be determined if the properties of the hinge are known. Eq. (7) yields:

$$h_1 = \sqrt{\frac{6S}{b}} \quad \text{and} \quad I_1 = S\sqrt{\frac{3S}{2b}} \tag{8}$$

Solving Eqs. (5) and (6) explicitly renders:

$$L_1 = r \frac{\beta_v - \beta_\alpha}{1 - \beta_\alpha} \quad \text{and} \quad h_2 = h_1 \left(\frac{1 - \beta_v}{\beta_\alpha(2 - \beta_\alpha) - \beta_v} \right)^{1/3} \tag{9}$$

where $\beta_\alpha = I_1/rK_\alpha$ and $\beta_v = 2I_1/r^2K$.

Finally, the length L_2 is obtained from (4) as:

$$L_2 = r \frac{1 - \beta_v}{1 - \beta_\alpha} \tag{10}$$

Note that α and v_x are of the same sign for the loading considered, which results in $0.5\beta < \beta_\alpha < \beta < 1$. This in turn secures that the dimensions of the equivalent beams can always be determined from formulae (8)–(10).

Table 1 gives the values of all the parameters involved for the hinge considered in Section 3. The first column lists the hinge dimensions, the second column shows the results calculated with the help of the 3D model. The third column was obtained using the definitions (1)–(3). Finally, the last column was calculated from (8)–(10).

Note that the heights h_1 and h_2 defining the equivalent beam are close to the height t . Also note that in order to model it by the FEM two beam elements defined by the pairs h_1, L_1 and h_2, L_2 , respectively, are needed. Clearly, to simulate the behavior of the entire hinge only four beam elements are required.

As indicated in Fig. 3, the link rotates and translates as a nearly rigid body. It is therefore postulated that the entire link can be modeled sufficiently by one beam element with the area and the area moment of inertia defined by $A = hb$ and $I = (1/12)h^3b$, respectively.

Consequently, the entire mechanism, which consists of hinges and links, can be represented by the beam elements. Note, however, that the beams representing the hinges have fictitious dimensions, while the beams representing the links have actual dimensions. Such a model will be referred to as the equivalent beam model (EBM), and will have a drastically reduced number of DOF. For example, the number of DOF in the EBM model used in the next section (that is computationally as accurate as 3D models) is about 160 times smaller than in its 2D counterparts, which in turn would be less accurate than the corresponding 3D models.

It worthwhile to mention that the EBM approach is different from the simplified pseudo-rigid body models that consist of springs and rigid links, as discussed in [11]. The right circular hinge in such a model would be represented by a pin joint with a rotational spring. The hinge's behavior would be characterized only by the spring's stiffness. Especially the hinge's length, lateral stiffness, and 3D effects related to its height-to-depth ratio are not represented in such models.

5. Validation of the EBM approach

The static and dynamic performance of the EBM is verified by three tests.

In Test I the EBM is compared to the 3D model of one hinge and parts of two links presented in Section 3. Test II examines the static and Test III the dynamic performances of the EBM that model the entire compliant mechanism shown in Fig. 1. These tests compare the static displacements of the end-effector under the actuator forces and the modal characteristics of the EBM with the mechanism modeled by 2D elements with either the plane stress or plane strain assumptions.

Table 1
Calculation of the equivalent beam geometry

Hinge properties	FEM data	Hinge parameters	Beam parameters
$b = 10 \text{ mm}$	$\sigma_y = 219.4 \text{ MPa}$	$S = 0.9116 \text{ mm}^3$	$h_1 = 0.7396 \text{ mm}$
$r = 1 \text{ mm}$	$v_x = 1.665 \times 10^{-3} \text{ mm}$	$K = 1.144 \text{ mm}^2$	$h_2 = 1.1434 \text{ mm}$
$t = 0.8 \text{ mm}$	$\alpha = 2.558 \times 10^{-3} \text{ rad}$	$K_\alpha = 0.7446 \text{ mm}^3$	$L_1 = 0.2496 \text{ mm}$
$M = 200 \text{ N mm}$			$L_2 = 0.7504 \text{ mm}$

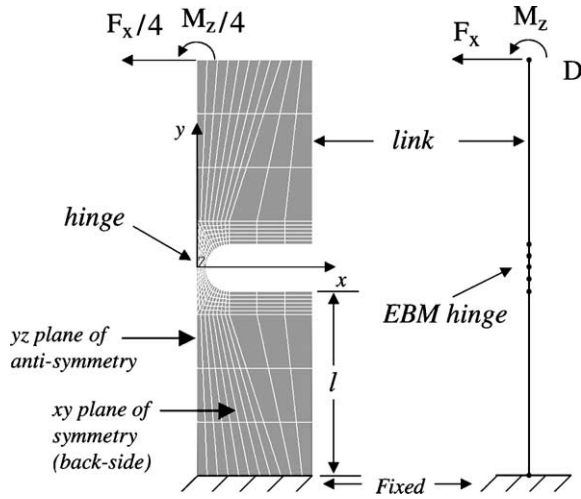


Fig. 5. Models to test EBM validity.

5.1. Test I

The main purpose of Test I is to check the EBM response to the lateral (shear) force. One should keep in mind that the equivalent beam parameters in Section 4 were developed using the standard Euler–Bernoulli theory of beams, which considers deformation due to pure bending only. The models shown in Fig. 5 are compared. The 3D model has about 48 000 DOF, while the corresponding EBM model has only 18 DOF. Only the xy -face of the 3D model is visible, there are 12 layers of elements in the z -direction.

The loading consists of moment M_z and force F_x combined in such a way that the bending moment at the section $y=0$ is the same as that used in Section 3, i.e. $M = M_z + F_x(l + r) = 0.2 \text{ N m}$. Not surprisingly, under a pure bending ($F_x = 0$) the slope of the end deflection v_x^D , the rotations α_z^D , and the maximum stresses in the both models are indistinguishable. The results start differing slightly if the shear force is present. The worst case occurs if $M_z = 0$ and only the lateral force $F_x = 22.22 \text{ N}$ is applied. The results of this worst case, which are shown in Table 2, indicate that the shear effects are in fact negligible.

Table 2
The EBM and the 3D models under the lateral force

Model result	EBM result	3D hinge result	% Difference
$\sigma_{y \max}$	219.4 MPa	219.2 MPa	0.1
v_x^D	$46.6 \times 10^{-3} \text{ mm}$	$46.5 \times 10^{-3} \text{ mm}$	0.3
α_z^D	$5.150 \times 10^{-3} \text{ rad}$	$5.116 \times 10^{-3} \text{ rad}$	0.7

The EBM mimics the behavior of the 3D model of the hinge very well. This confirms that the beam models of the hinge and links are accurate. It is noteworthy to mention that much less effort is required to set-up and build the model using the EBM versus the 3D modeling approach; further, the EBM model takes fractions of a second to solve compared to the minutes required to solve the 3D model.

The analyses have been repeated for the models with different l/r ratios resulting in similar results. Even if $l \rightarrow 0$, that is with no link and the lateral force applied directly to the hinge, the EBM and the 3D results were never different by more than about 2%.

5.2. Test II

This test compares the static behavior of the EBM of the entire 3RRR mechanism to a planar model of the same mechanism built of 2D elements under the assumption of either the plane-strain state or the plane-stress behavior. Since the plane stress and the plane strain states give the lower and upper limits of the mechanism stiffness, it is expected that the EBM model results will lie between the results of the aforementioned 2D models. It should be noted that a complete 3D model of the whole compliant mechanism would require a substantial numerical effort.

Some identical idealizations have been used in all the models to make the comparison meaningful. Namely, the fixed base (the centrepiece) of the mechanism (see Fig. 1) is assumed to be completely rigid. Consequently, the ends of the hinges that are attached to the centrepiece are fixed as shown in Fig. 6.

The piezoelectric (PZT) actuators are placed between the fixed base and the links referred to as the PZT blocks. The actuation forces, parallel to the actuators' axes, are applied to the PZT blocks, which cannot rotate but are free to deflect in the transverse directions. Both the 2D planar and EBM models are actuated in the same way.

The end-effector is represented by a mass element placed at point O (the origin of the x – y coordinate system). The mass and mass-moment of inertia for the element are identical as the mass and the mass-moment of inertia of the circular plate constituting the end-effector. This element is interfaced to the compliant mechanism using a number of stiff but massless beam elements. The stiffness of these elements was selected in such a way that they rotate and translate with the mass element as one rigid body.

The model is actuated by forces F_i that can be exerted on any of the PZT blocks numbered as 1, 2 and 3. To ensure that

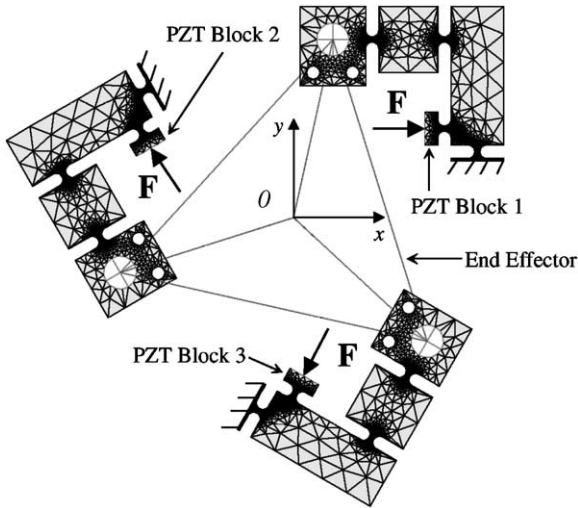


Fig. 6. The 2D model of the 3RRR mechanism.

the load is properly distributed several stiff beam elements imitating the actuator's surface were attached to the edge of each PZT block where the forces are applied.

The 2D model of the 3RRR mechanism was meshed with quadratic planar elements available from the ANSYS program, namely: 6-node triangular elements *PLANE2*, and 8-node quadrilateral elements *PLANE82*. Details of the meshing of the hinge are shown in Fig. 7. This model has about 46 500 DOF. Either the plane-stress or plane-strain states can be selected by setting an appropriate key-option in the ANSYS program.

The corresponding EBM model of the 3RRR mechanism is built entirely with the 2D beam elements *BEAM3*. The flexure hinges are modeled by the beam elements sized as discussed in the previous section. The links between the flexure hinges are modeled as beams based on their true dimensions. The end-points of the flexure hinges attached to the centrepiece and the end-effector are modeled identically as in the planar model.

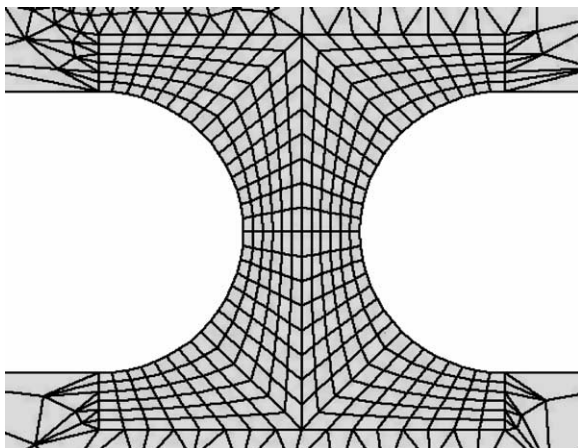


Fig. 7. Meshing of the hinges of the planar models.

Some intermittent beam elements are used to close any offset created when the beams modeling the hinges and links do not meet end to end. These elements have stiffness equivalent to that of the particular missing link.

The EBM model of the mechanism is shown in Fig. 8 with the ghosted 2D model to aid in the visualization. The whole EBM model has 291 DOF, which is approximately 160 times less than its planar counterpart.

In order to compare the models, three load cases were used. In all the cases a constant load of 250 N was applied to the PZT blocks in the combinations as follows:

- Case 1: PZT block 1 is loaded.
- Case 2: PZT blocks 1 and 2 are loaded.
- Case 3: PZT blocks 1, 2, and 3 are loaded.

Of interest from the models are the end effector's translations (in the *x*- and *y*-directions) and rotation, and the maximum stresses developed.

Also, the deformation patterns of the entire mechanism models were compared graphically after each test case. The example of such a comparison is presented in Fig. 9 for the load of Case 3. The figure is actually a combination of two plots taken from the EBM model and the 2D plane strain model. The displacement scaling of these plots is 50-fold. It is seen that the deformation of the EBM model of the 3RRR mechanism appears to be indistinguishable.

For each load case the resulting end-effector motion and the maximum stress as obtained from the three models are listed in Table 3. The translations of the end-effector centre (point O) are denoted by v_x and v_y , while its angle of rotation by θ .

Note that the end-effector displacements predicted by the EBM model fall between the results of the plane strain and plane stress model (an exception is v_y for case I, however, the value of this displacement component is only about 1% of the displacement in the *x*-direction, i.e. $|v_y| \approx 0.01v_x$). Fur-

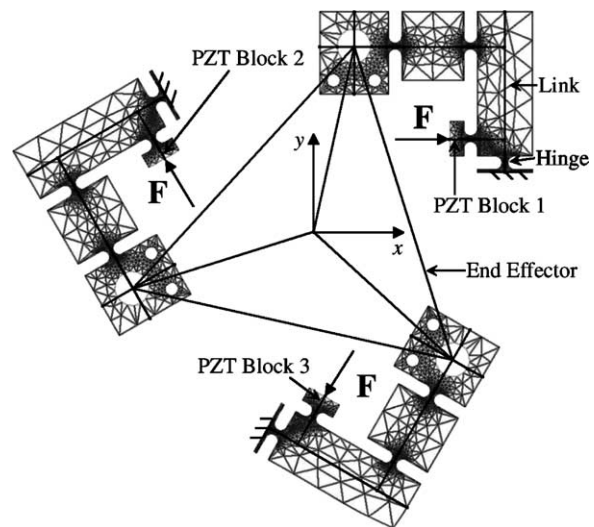


Fig. 8. The graphical representation of the EBM model of the mechanism.

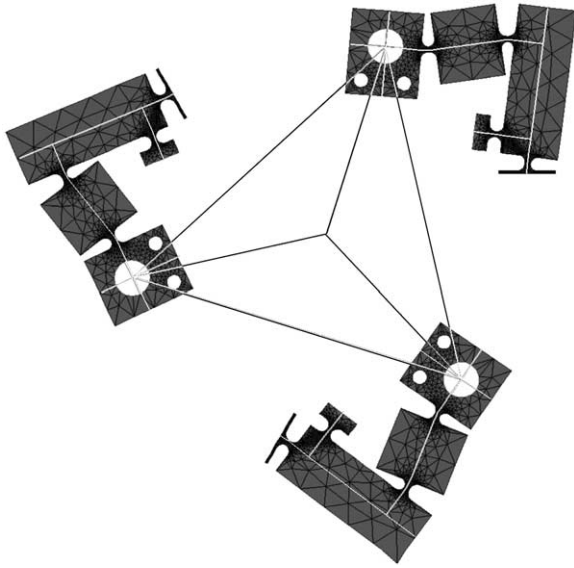


Fig. 9. The deflection patterns of the EBM and 2D plane strain models.

ther, the relative errors, as shown in brackets, agree well with the results presented in Fig. 4, which indicate that the stiffness of a hinge assuming the plane strain state are approximately 1.8% higher than the 3D stiffness, and that a hinge assuming the plane stress state were approximately 8.6% lower.

The maximum stresses in the EBM model are roughly 2% greater than those obtained from either of the 2D models. This agrees well with the difference between the stress in the 3D model of the hinge and the corresponding 2D models as mentioned in Section 3 and indicates that the EBM’s stress results are more accurate than the results obtained from either 2D models.

In summary, Test II shows that the EBM is capable of simulating the static characteristics of flexure hinges and the whole 3RRR compliant mechanism accurately with a very low number of DOF. It opens new possibilities of formally optimizing such mechanisms. Typical numerical optimization procedures require a large number of analyses to establish

sensitivities to various design parameters and therefore are impractical for complex FEM models. With the EBM model the entire mechanism’s topology as well as the stiffnesses of individual hinges and links can be improved.

The EBM can also be used in dynamics and possibly in a real time control environment (the model is solved in less than 1 s on a 800 MHz processor). In order to indicate its usefulness for dynamic considerations the results of the modal analysis are presented in the next section.

5.3. Test III

The last test is designed to check whether the EBM is also capable of simulating the dynamic characteristics of the mechanism. We assume that the compliant mechanism, such as the 3RRR mechanism, can be simulated by the linear FEM model and then solved by the mode superposition dynamic procedures. It implies that two models can be considered dynamically similar if their modal characteristics are similar. In practice, only several lowest frequencies and the corresponding modal shapes of two different structures need be close to securing their almost identical dynamic responses to a large variety of loadings.

It is assumed that the compliant links and hinges are made of brass alloy ($\rho = 8750 \text{ kg/m}^3$), while the end-effector is made of steel ($\rho = 7800 \text{ kg/m}^3$). The end effector is modeled by one mass element (MASS21) with the mass and mass moment of inertia of a circular steel plate. This element is attached though a number of rigid and massless beam elements in a triangular pattern to the links as can be seen in Figs. 6, 8 and 9. The masses of the links and hinges in the EBM and 2D models are identical. The standard modal analysis of both models was completed using the subspace iterations procedure with the ANSYS program. Again, the 2D elements were used with either the plane stress or plane strain options. The EBM model has 291 DOF, while the 2D models have about 46 500 DOF. The first four eigenfrequencies obtained from these models are listed in Table 4.

The frequencies of the first two modes are identical because of a ‘tri-symmetry’ of the 3RRR mechanism. As it can

Table 3
Results of Test II

Load case	Result	EBM	Plane strain	Plane stress
1	v_x (μm)	32.5	31.8 (−2.1%)	35.6 (+9.5%)
1	v_y (μm)	−0.4	−0.5	−0.5
1	θ (mrad)	−0.56	−0.55 (−1.8%)	−0.62 (+9.8%)
1	σ_{eqv} (MPa)	191	189 (−1.3%)	189 (−1.1%)
2	v_x (μm)	16.6	16.3 (−1.63%)	18.2 (+10.0%)
2	v_y (μm)	27.9	27.3 (−2.3%)	30.5 (+9.3%)
2	θ (mrad)	−1.13	−1.11 (−1.76%)	−1.24 (+9.8%)
2	σ_{eqv} (MPa)	316.4	308 (−2.8%)	308 (−2.5%)
3	v_x (μm)	0	0	0
3	v_y (μm)	0	0	0
3	θ (mrad)	−1.69	−1.66 (−1.76%)	−1.82 (+9.85%)
3	σ_{eqv} (MPa)	232.4	228 (−2.1%)	228 (−1.8%)

Table 4
Results of the modal analysis (frequencies in Hz)

Mode	EBM	2D plane stress	2D plane strain
1. Translational	436.8	423.8 (−2.97%)	447.2 (2.37%)
2. Translational	436.8	423.8 (−2.97%)	447.2 (2.37%)
3. Rotational	640.6	618.6 (−3.43%)	652.3 (1.84%)
4. Local	12500	12038 (−3.70%)	12683 (1.46%)

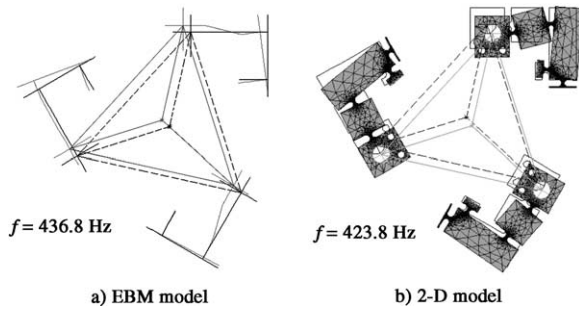


Fig. 10. The first mode of vibrations (translational).

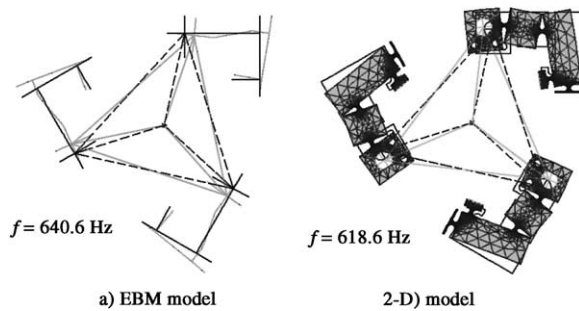


Fig. 11. The third mode of vibrations (rotational).

be seen the results of the EBM model are always bound by those of the 2D plane stress and plane strain models. It is believed, that the EBM results would be very close to the results that would be obtained from a hypothetical 3D model of the mechanisms with a sufficiently large DOF number (perhaps millions).

Also, the modal shapes show an excellent agreement. Figs. 10 and 11 show the first and the third modes of vibrations obtained from the EMB (a) and 2D plane stress (b) models.

Again, it is noteworthy to mention that it takes a fraction of a second to solve the EBM for 20 modes, while it becomes incomparably long (about 10 min on 800 MHz processor) to solve either of the 2D planar models. Also, it should be mentioned that modeling the links in the EBM by one beam element is sufficient for the static analysis and for simulating several lowest modes of vibrations. However, if a wide spectrum of eigenfrequencies is required the links should be meshed with more than one element.

6. Conclusions

In order to be accurate, the FEM modeling of typical planar compliant mechanisms should be capable of including the 3D nature of the stress/strain in flexure hinges. It necessitates a wise use of available elements if one wants to avoid generating somewhat impractical FEM models with prohibitively large number of DOF. As shown in the paper, the static and dynamic characteristics of the whole 3RRR mechanism can be simulated with high precision with a model that has a very small number of DOF. The EBM model developed accurately predicts the displacements of the end-effector, the maximum stress, and the modal characteristics of the mechanism. It has been achieved mainly by replacing the flexure hinges by equivalent beams of identical mechanical characteristics. The numerical efficiency of the EBM model is very high. Therefore it becomes conceivable to apply it for other purposes such as mathematical optimization, simulating complex dynamic responses, or even for real time applications to control and handling of compliance mechanisms.

References

- [1] Zhang S, Fasse ED. A finite-element-base method to determine the spatial stiffness properties of a notch hinge. *J Mech Des* 2001;123:141–7.
- [2] Her I, Chang JC. A linear scheme for the displacement of micro-positioning stages with flexure hinges. *J Mech Des* 1994;116:770–6.
- [3] Ragulskis KM, Arutunian MG, Kochikian AV, Pogosain MZ. A study of fillet type flexure hinges and their optimal design. *Vib Eng* 1989;3:447–52.
- [4] Smith ST, Badami VG, Dale JS, Xu Y. Elliptical flexure hinges. *Rev Sci Instrum* 1997;68(3):1474–83.
- [5] Xu W, King T. Flexure hinges for piezoactuator displacement amplifiers: flexibility, accuracy, and stress considerations. *Prec Eng* 1996;19:4–10.
- [6] Lobontiu N, Paine JSN, Garcia E, Goldfarb M. Corner-filletted flexure hinges. *J Mech Des* 2001;123:346–52.
- [7] Paros JM, Weisbord L. How to design flexure hinges. *Mach Des* 1965;37:151–6.
- [8] Rong Y, Zhu Y, Lou Z, Liu X. Design and analysis of flexure-hinge mechanism used in micro-positioning stages. *Manuf Sci Eng* 1994;PED-68(2):979–85.
- [9] Ryu JW, Gweon D-G. Error analysis of a flexure hinge mechanism induced by machining imperfection. *Prec Eng* 1997;21:83–9.
- [10] Zettl B. Effective finite element modelling of micro-positioning systems. M.Sc. Thesis. Dep. Mech. Eng., University of Saskatchewan, 2003.
- [11] Howell LL. Compliant mechanisms, Chapter 5. Pseudo-rigid-body model. Wiley-Interscience; 2001.